# ACOUSTIC EMISSION RESPONSE OF E-GLASS/POLYESTER WOVEN ROVING COMPOSITE

**Khalil M. Elawadly, E.A. Esmail, M.S. Abou Elwafa**
Mathematical Engineering and Engineering Physics Department, Faculty of Engineering, Alexandria University, Alexandria 21544, Egypt.

and **J.P. Blanchard**
Nuclear Engineering and Engineering Physics Department, University of Wisconsin-Madison, U. S. A.

ABSTRACT

Tensile failure mechanisms in E-glass/Polyester woven roving composite have been studied using acoustic emission (AE) technique. The results indicate that the AE rms voltage and the cumulative AE count are able to analyze the behavior of the fiber reinforced composite materials under tension. Also, AE technique can predict first ply failure and matrix cracking or debonding between the fiber and the matrix ( slipping). This technique shows great promise as a non-destructive testing technique (NDT) for composite materials since it gives a complete information about all mechanisms which may occur during testing.

*Keywords : Acoustic Emission, Composite materials, E-glass/Polyester, Woven Roving, Failure Mechanism.*

## INTRODUCTION

Several methods have been used to monitor the damage occurrences in composites. Among these, the technique of acoustic emission ( AE ) has been increasingly used. AE is based on monitoring the stress waves that are generated by rapid local redistributions of stress which accompany the operation of many damage mechanisms. Because of the composite materials, the modes and criteria for deformation and fracture processes are very complex. Acoustic emission techniques can be used to establish the deformation and fracture modes operative during the straining of a composite material. This behavior is particularly important when the composite material is to be used in a hazardous or aggressive environment, at elevated or low temperatures, or under alternating load conditions.

In most material systems the local instabilities frequently dictate the criteria for deformation and fracture processes, as, for example, in the region in the immediate vicinity of a crack which undergoes elongation and plastic deformation from localized high stresses. Knowledge of this propagation would be significant in an integrity evaluation of the material or component. In this situation the crack would be the generator or source of acoustic emission activity and would herald imminent catastrophic failure.

Dunegan et all [1] have proposed a measurable relationship which exists between acoustic emission and the stress intensity factor. A theoretical model was developed which predicts that the total acoustic count from a specimen with a sharp crack should be proportional to the fourth power of the stress intensity factor. This model predicts the total acoustic emission count as a function of stress intensity factor, and is based on some assumptions such that the acoustic emission rate reaches a maximum when strain levels approach yielding. In another work Dunegan [2] has shown that a fit between Gilman's mobile dislocation model and the acoustic emission rate curve is possible for certain metals. Gilman's equation for mobile dislocation density is

$$N_m = (N_o + m_p \epsilon_p) e^{-\phi \epsilon_p} \quad (1)$$

where $N_m$ is the mobile dislocation density, $N_o$ is the number of initially mobile dislocations, $m_p$ is the multiplication factor, $\varepsilon_p$ is the plastic strain, $\phi = H/\sigma$ where H is the work-hardening coefficient, and $\sigma$ is the root mean square shear stress. Assuming that $N_o = 0$, due to dislocation locking in high strength materials, the coefficient $\phi$ can be evaluated by observing the strain at which the peak in acoustic emission rate occurs. The above equation shows that the ring-down counting number is proportional to the strained volume of the unflawed specimens. This shows that each AE burst is due to co-operative motion of big number of dislocations.

The various stages of microcrack initiation, microcrack growth, and final fracture have been described by Tetlman and Chow [3]. They also discussed theoretical relationships between these processes and acoustic emission response. They developed an expression which predicts emission count as a function of stress level. Unfortunately, the microstructural complexity of composite materials and the diversity of types of composites that are known make it difficult to apply to different composites the same AE monitoring procedures that have worked satisfactory for metals.

Low level acoustic emissions can be generated by the plastic deformation of the matrix or the fibers. Sources of large, burst-type emissions are fiber failure, gross matrix cracking, interface failure, or fiber pullout. Also AE may arise from known and sometimes unknown structural flaws such as intralaminar and interlaminar cracks, and from stress concentrations such as at re-entrant corners. Extraneous AE-noise sources are a particular problem for AE applied to composite material scientific studies. Without some modifications, most composite test samples generate significant extraneous AE.

Most theories of tensile failure of fiber reinforced composite consider only the strength properties of the fiber. Harris et al.[4] derived an equation relating the percentage of cracked fibers to the cumulative AE count which gave good agreement with the experimental data within a constant scale factor. Experimental results by Zweben and Rosen [5] support the cumulative fracture propagating concept. A comparison of theoretical and experimental work supports the cumulative fracture mode. Guild et al [6] studied the behavior of glass/polyester composites of various kinds and they have been assessing the use of AE amplitude analysis as a means of obtaining information relating to micromechanisms of failure in glass reinforced plastic (GRP). Henneke et al. [7] were able to identify a sharp increase in the AE count rate which corresponded to the kink of the bilinear stress-strain curve for a laminate with boron reinforced epoxy face sheets and an aluminum core. This is despite the fact that they were able to state that the increased emissions were associated with fiber or matrix fracture, fiber-matrix debonding, or delamination of the composite face sheets from the aluminum core. Takehana and Kimpara [8] showed that for a variety of woven structures in glass polyester composites, significant changes in AE could be associated with kinks in the stress-strain curve. Hamstad and Chiao [9] showed how an AE record was used to identify a graphite/epoxy pressure vessel which had been wound with frayed fiber. It is also possible to predict failure in composite laminates from basic laminae properties and a knowledge of the stacking sequence. In particular, to predict fiber failure or transverse failure in composite laminates it is common to use anisotropic strength criteria. The maximum stress and maximum strain criteria, the Tsai-Hill criterion and the Tsai-Wu criterion are commonly used to predict the strength of the laminate on the basis of the strengths of the individual plies within the laminates. A relatively little understood mode of failure of composite laminates is the delamination which means failure of the interface between two adjacent plies [10]. White and Tretout [11] used AE monitoring to study the failure mechanism in carbon-fiber reinforced epoxy plates subjected to bending. Applying frequency analysis to the AE signal, they found different frequency signatures for the different modes of failure. In this paper, the acoustic emission (AE) technique will be used to analyze the failure mechanisms in E-glass/ Polyester woven roving composite.

## APPARATUS

Figure (1) shows a detailed construction of the tensile test system designed to work with low noise since it uses the buoyancy force for loading and load

release. Buoyancy force technique was used to solve the noise problem which may appear from the mechanical friction. Two water tanks were used, the inner one filled with water to a prescribed level floats inside the outer one. Once the water level inside the outer tank is dropped, the difference between the buoyancy force at the weight of the inner tank gives the required load.

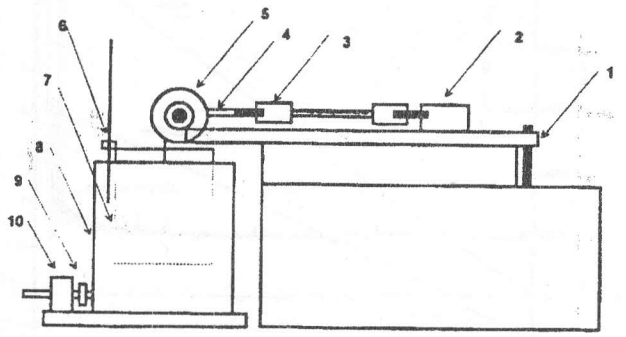


Figure 1. Schematic diagram of the tensile testing system.

Figure (2) shows the block diagram of the acoustic emission detection and measuring system. It is important to minimize the background noise during acoustic emission tests. So, the tensile testing machine must be checked for noise. The root mean square volt of the acoustic emission, the applied load, the acoustic emission count, and the elongation of the specimen were plotted simultaneously using two T-YY recorders.

## SPECIMEN GEOMETRY

The specimen is fabricated from woven roving fiber glass/polyester layered composite laminates with fiber volume fraction of 60 % and is tabbed with cross-plies tabs. In this study two patterns of fiber orientation $[0°/90°]_n$ and $[+45°/-45°]_2$, are used. Figure (3) represents a schematic diagram of the specimen and the clamp which used in this study. An inherent difficulty in such test is the need to reduce nonuniformity in the stress field due to the end constraints. The first method to reduce this difficulty is to make the specimen slender by reducing the gage length to width ratio to less than twelve [12,13]. The second method is to allow rotation of the tabs by means of a hinge or pin. A specimen width of 15 mm and thickness of 2 mm for the two layer specimens and 3 mm for the three layer specimens were chosen for this study, at the same time the clamp was designed with the ability to rotate to overcome any difficulty in the stress distribution specially in the off-axis test, i.e. $[+45°/-45°]_2$. Table 1 shows the engineering elastic properties of the E-glass/polyester laminated woven roving composite material [14]. All samples have fiber volume fraction of 60% .

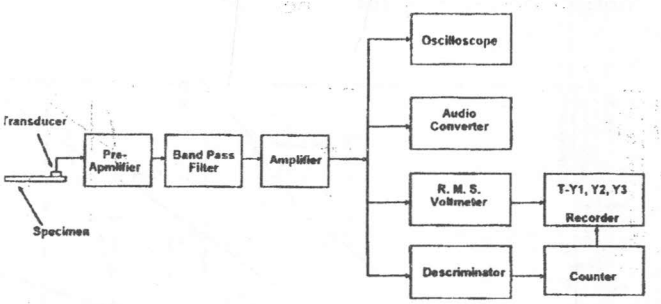


Figure 2. Block diagram of the acoustic emission detection and measuring system.

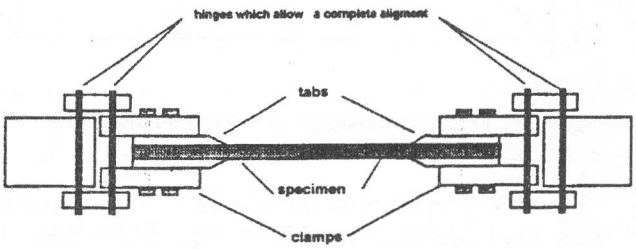


Figure 3. Schematic diagram of the specimen and the clamp.

## RESULTS AND DISCUSSION

The emission generated during the loading of the specimens have been monitored in order to detect damage occurring within the specimen. An amplification gain has been used to be sure of excluding any electric noise, inherent in the system,

from the count.

Figure (4) shows typical results of the tension test for a specimen with fiber orientation of $[0°/90°]_3$. It is obvious from this figure that the acoustic emission starts to appear from the beginning of the test. The cumulative acoustic emission count increases rapidly at the matrix cracks then followed by a step change as shown in the figure. Also, the same behavior can be noticed in the AE rms voltage curve. The elongation curve shows a change in the slope (knee) at about 2350 N applied force corresponding to a stress of 78.33 MPa, indicating that the matrix lost its strength and the fiber will put on more contribution to carry the applied load. The knee of the elongation curve occurs at the yield point of the matrix, which is the translation point between the elastic and plastic region, and this behavior can be noticed in most of the specimens.

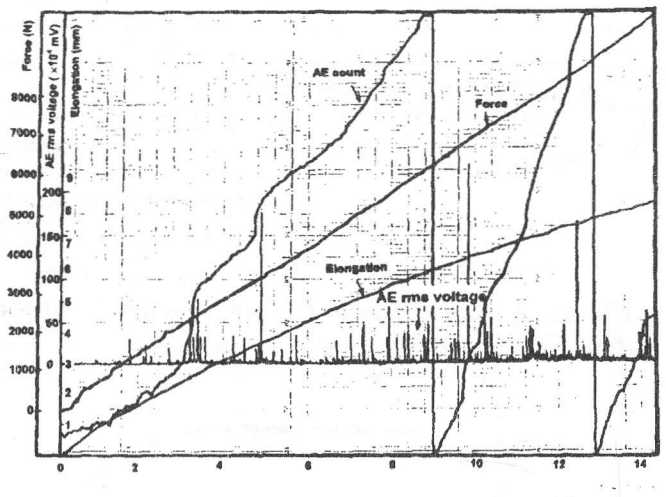


Figure 4. Force, cumulative acoustic emission, and AE rms voltage against time (fiber orientation $[0°/90°]_3$).

Figure (5) represents the test results for a specimen with fiber orientation of $[0°/90°]_2$. The value of the ultimate stress at failure for this specimen is 211.88 MPa accompanied by a maximum strain of 1.75% . The value of the AE rms voltage was dramatically increased at a tensile force of 5780 N, indicating the beginning of slipping between the fiber and the matrix (debonding) which could be seen by visual inspection during the test. The knee in the elongation curve for this specimen is observed at a stress equal to 78 MPa at which a first ply failure occurs, accompanied by a sharp increase in the acoustic emission count and also a peak in the AE rms voltage curve, as seen in the figure. After the first ply failure the number of cracks in the matrix increases, indicating the onset of edge delamination.

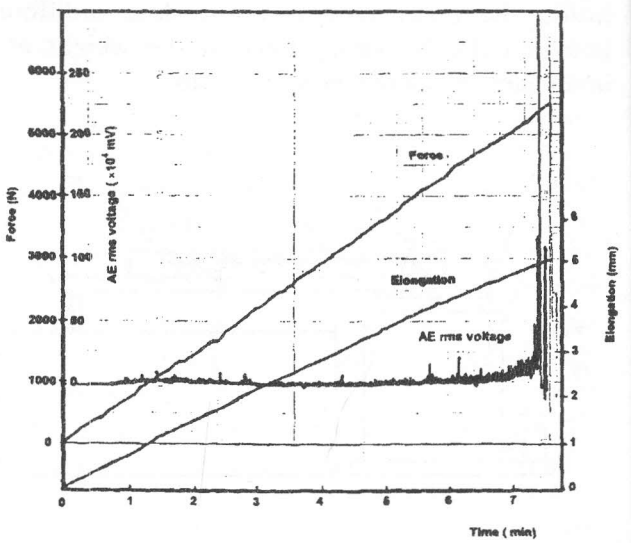


Figure 5. Force, elongation, and AE rms voltage against time (fiber orientation $[0°/90°]_2$).

Figure (6) shows the results for another specimen with fiber orientation of $[0°/90°]_2$. This figure shows two large peaks at forces equal to 4620 N and 5200 N respectively. These peaks were accompanied by a creation of a matrix cracking at two locations in the specimen. The stress of failure for this sample was 192.63 MPa, which means that the matrix crack leads to reducing the strength of the specimen, indicating fiber failure mechanisms without slipping. The matrix crack is accompanied by a noticeable change in the elongation curve which indicate that the fiber suffer from a sudden strain after the matrix failure.

Figures (7) and (8) represent the results of the specimens having orientation $[\pm 45°]_2$ laminate. It is obvious from these figures that no significant AE activity observed or recorded before ultimate failure. A small change in the AE rms voltage curve occurs only at the moment of failure. At the same time this group shows that a large amount of plastic deformation in shear precedes ultimate failure. The maximum strain at failure for this group is about 1.7 times the value obtained for the first group ($[0°/90°]_2$ laminate).

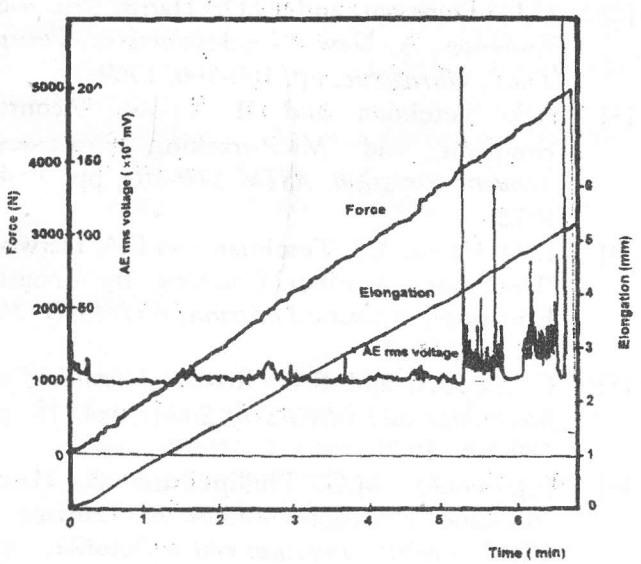


Figure 6. Force, elongation, and AE rms voltage against time (fiber orientation $[0°/90°]_2$).

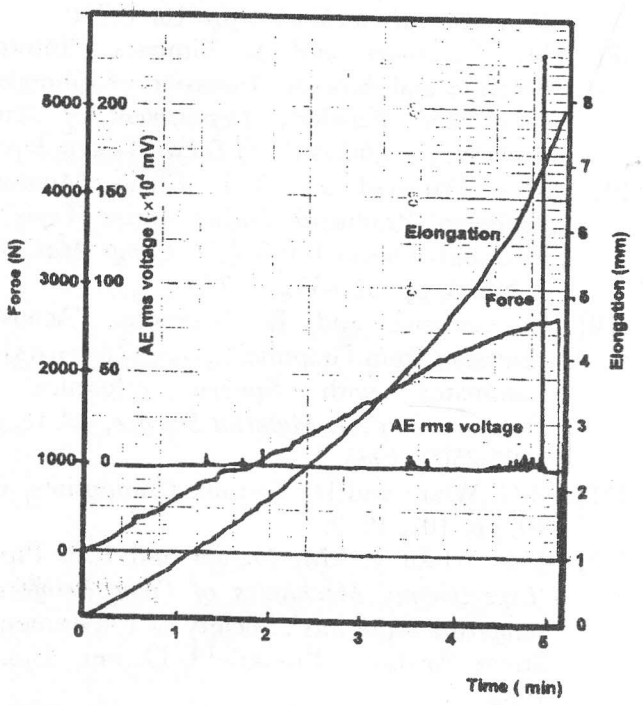


Figure 7. Force, elongation, and AE rms voltage against time (fiber orientation $[\pm 45°]_2$).

In the specimens with fiber orientation $[0°/90°]_2$ laminate, two distinct regions are seen in the AE rms voltage and the cumulative AE count data during deformation. An initial rise in the peak value of the AE rms and a corresponding sharp increase in the cumulative AE count apparently corresponding to the first ply failure followed by approximately sudden increase in the cumulative AE count. A region with rapid increase in AE activity is indicated by high peaks in the AE rms voltage with increase in slope of the cumulative AE count. This increase is due to the onset of edge delamination as seen by visual inspection during deformation.

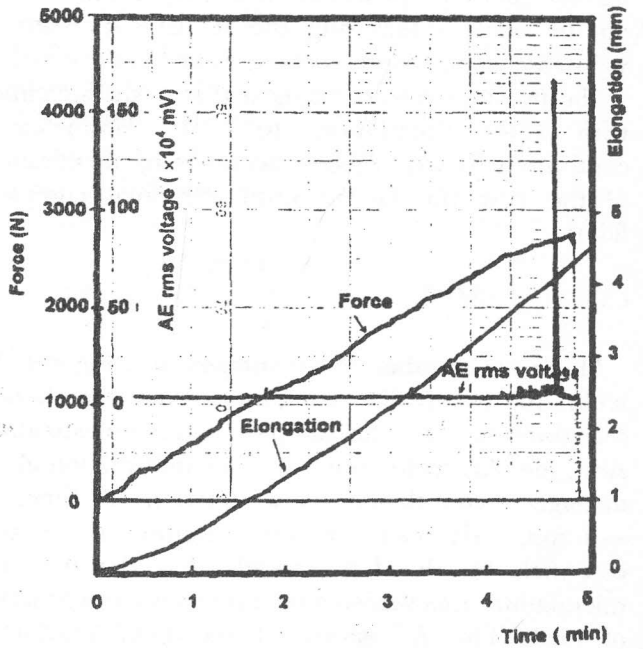


Figure 8. Force, elongation, and AE rms voltage against time (fiber orientation $[\pm 45°]_2$).

According to the above results, the matrix crack is always accompanied by a release of a large amount of energy which is remarkable in the AE rms voltage curve with a sharp peak. It is also clearly noticed that after the yield point, the number of mobile dislocation in the matrix increases and a plastic deformation starts to appear which leads to an increase, at a high rate, in the count number of acoustic emission produced through the test. In the specimens with fiber orientation $[\pm 45°]_2$ laminate, a large amount of plastic deformation in shear causes ultimate failure. No significant AE activity was recorded before ultimate failure. Also, in this group, neither edge delamination nor matrix cracking was observed.

The acoustic emission energy can be calculated from the equation

$$E = K \Sigma A^2 dt \qquad (2)$$

where E is the AE energy, K is constant depending on the measuring instruments, and A is the amplitude of the rms voltage of AE. For the composite materials the rms voltage plot has very sharp growing and decaying patterns with extremely narrow duration, for which the above summation can not be made. Measuring the acoustic emission in such case needs more sophisticated instruments.

The previous results suggest that in the specimen with fiber orientation $[0°/90°]_n$ laminates a continuous damage process occurs from the initiation of the first ply failure until the final complete failure.

## CONCLUSION

There are number of advantages of using the AE technique to test fiber composites. One can obtain a real time data for the samples under investigation. Also, the AE technique provides information about damage accumulation as a function of time. In addition, AE can provide unique information essential to develop models for damage and microfailure mechanisms in composites as a function of load. The AE study of the fiber reinforced composite materials gives a good information about basic failure mechanisms of these materials. The AE rms voltage and the cumulative AE count obtained in this make it possible to analyze the behavior of the fiber reinforced composite materials under tension. Also, AE technique can predict first play failure and matrix craor debonding between the fiber and the matrix ( slipping). This technique shows a great promise as a non-destructive testing technique ( NDT ) for composite materials since it gives a complete information about all mechanisms which may occur during the process.

## REFERENCES


[1] H.L. Dunegan, D.O. Harris and C.A. Tatro, "Fracture Analysis by Use of Acoustic Emission", *Engineering Fracture Mechanics*, vol. 1, pp. 105-122, 1969.

[2] H.L. Dunegan and D.O. Harris, "Acoustic Emission A New Nondestructive Testing Tool", *Ultrasonic*, pp. 160-166, 1969.

[3] A.S. Tetelman and R. Chow, "Acoustic Emission and Microcracking Processes", *Acoustic Emission, ASTM STP-505*, pp. 30-40, 1972.

[4] D.O. Harris, A.S. Tetelman and F.A. Darwish, "Detection of Fiber Cracking by Acoustic Emission", *Acoustic Emission, ASTM STP 505*, pp. 238, 1972.

[5] C. Zweben and B.W. Rosen, *Journal of the Mechanics and Physics of Solids*, vol. 18, pp. 189-206, 1970.

[6] F.J. Guild, M.G. Phillips and B. Harris, "Acoustic Emission Studies of Damage in GRP", *NDT International*, October, pp. 209-215, 1980.

[7] E.G. Henneke II, C.T. Herakovich, G.L. Jones and M.P. Renieri, "Acoustic Emission from Composite-Reinforced Metals", *Experimental Mechanics*, pp. 10, 1975.

[8] M. Takehana and I. Kimpara, "Internal Fracture and Acoustic Emission of Fiberglass Reinforced Plastics", *Department of Naval Architecture, University of Tokyo*, Tokyo, Japan.

[9] M.A. Hamstad and T.T. Chiao, "Acoustic Emission Produced during Burst Tests of Filament-Wound Bottles", *J. Comp. Mat.*, vol. 7, No. 3, pp. 320-332, 1973.

[10] L. Carlsson and B. Norrbom, "Acoustic Emission from Graphite/Epoxy Composite Laminates with Special reference to Delamination", *J. Material Science*, vol. 18, pp. 2503-2509, 1983.

[11] R.G. White and H. Tretout, Composites, vol. 10, pp. 101, 1979.

[12] J.M. Whitney, I.M. Daniel and R.B. Pipes, "*Experimental Mechanics of Fiber Reinforced composite Materials*", Society of Experimental Stress Analysis, Brookfield Center, U.S.A., 1982.

[13] S.M. Cron, A.N. Palazotto and R.S. Sandhu, "The Improvement of end- Boundary Conditions for Off-axis Tension Specimen Use", *Experimental Mechanics*, vol. 28, No. 1, March, pp. 14-19, 1988.

[14] Palatal A 410, technical Leaflet, M 2175, S1261, April, 1987.